

Evaluation of (α, n) Induced Neutrons as a Background for Dark Matter Experiments

D.-M. Mei^{a,*}, C. Zhang^{a,b}, A. Hime^c

^a*Department of Physics, The University of South Dakota, Vermillion, South Dakota 57069*

^b*College of Sciences, China Three Gorges University, Yichang 443002, China*

^c*P-23, H803, Los Alamos National Laboratory, Los Alamos, New Mexico 87545*

Abstract

Neutrons from (α, n) reactions through thorium and uranium decays are important sources of background for direct dark matter detection. The neutron yields and energy spectra from a range of materials that are used to build dark matter detectors are calculated and tabulated. In addition to thorium and uranium decays, we found that α particles from samarium, often the dopant of the window materials of photomultiplier tubes (PMT), are also an important source of neutron yield. The results in this paper can be used as the input to Monte Carlo simulations for many materials that will be used for next generation experiments.

Key words: (α, n) neutrons, Dark matter detection

PACS: 13.85.Tp, 23.40-s, 25.40.Sc, 28.41.Qb, 95.35.+d, 29.40.Wk

1 Introduction

Neutron induced elastic scattering processes represent an important background for direct dark matter detection experiments searching for Weakly Interacting Massive Particles (WIMPs), which may constitute the dark matter in the universe [1,2,3,4]. Direct searches for WIMPs have been carried out by many experiments including CDMS [5], EDELWEISS [6], Xenon10 [7], ArDM [8], DAMA [9], CRESST [10], PICASSO [11], NAIAD [12], and ZEPLIN [13]. Among these experiments, DAMA/Nai [14] and DAMA/LIBRA [15] have

* Corresponding author.

Email address: dongming.mei@usd.edu (D.-M. Mei).

claimed that they have observed a model independent annual modulation signature. The DAMA collaboration interprets this annual modulation as the signature induced by dark matter (DM) particles [14,15]. However, this claim is at odds with other experimental results if one assumes standard WIMP interactions and halo models. With the best limits set by CDMS II [16] and Xenon10, WIMPs remain unobserved. Large scale next generation detectors utilizing noble liquids to continue the direct search for WIMPs are underway. The key to these experiments lies in the ability to reduce various background to unprecedented low levels. Among all possible sources of background, neutron induced nuclear recoil is identified as a major source of background for this type of experiments.

There are three sources of underground neutrons: 1) those produced by (α, n) reactions through thorium, uranium, and other radioactive isotope decays in the materials that surround or constitute the detector; 2) those from spontaneous uranium fission; and 3) those from cosmic ray muon-induced processes. In general, the (α, n) neutrons dominate the total neutron contributions to the measured background for an underground experiment. This is because the origins of (α, n) neutrons range from surrounding rock, external shielding, inner shielding, detector components, and detector target. In particular, the (α, n) neutrons produced in the detector components and target are hard to cope with. These neutrons need to be understood very well in terms of their origin, transport, and interaction with materials. Calculations of the neutron yield and neutron energy spectrum in different materials are critical to dark matter experiments. The total neutron yield indicates the number of neutrons that enter or are produced in the target. The neutron energy spectrum determines the total background events in the region of interest (ROI). Therefore, a full simulation of neutron background must take into account both neutron yield and energy spectrum. This paper is aimed at providing the (α, n) neutron yield and energy spectrum for a number of materials that are used for the construction of dark matter detectors.

2 Calculations of neutron yields and energy spectra

The neutron yields from the (α, n) reaction for various elements of natural isotopic concentrations have been discussed by many authors [17,18,19,20,21,22,23,24,25,26,27,28,29,30]. The decays of ^{238}U and ^{232}Th in the materials produce MeV α particles. These α particles interact with the nucleus in a thick target and yield neutrons. The neutron yield is calculated by [21]:

$$Y_i = \frac{N_A}{A_i} \int_0^{E_0} \frac{\sigma_i(E)}{S_i^m(E)} dE, \quad (1)$$

where E_0 is the initial energy of the α -particle, S_i^m is the mass stopping power of element i , A_i is the atomic mass of element i and N_A is Avogadro's constant. In secular equilibrium, the ^{232}Th decay chain yields 6 α 's and the ^{238}U decay chain produces 8 α 's with various energies E_j . The neutron yields in the decay chains of ^{232}Th and ^{238}U can be determined by the sum of the individual yields induced by each α , weighted by the branching ratio for each element and weighted by the mass ratio in the host material. The energy attenuation of the α -particles in the medium is the dominant process for the thick target hypothesis. Under the assumption that the incident flux of α -particles with energy of E_j is invariant until the energy is attenuated to zero, for target element i , the differential spectra of neutron yield can be expressed as

$$\begin{aligned} Y_i(E_n) &= N_i \sum_j \Phi_\alpha(E_j) \int_0^{E_j} \frac{d\sigma(E_\alpha, E_n)}{dE_\alpha} dE_\alpha \\ &= \frac{N_A}{A_i} \sum_j \frac{R_\alpha(E_j)}{S_i^m(E_j)} \int_0^{E_j} \frac{d\sigma(E_\alpha, E_n)}{dE_\alpha} dE_\alpha, \end{aligned} \quad (2)$$

where N_i is the total number of atoms for the i^{th} element in the host material, $\Phi_\alpha(E_j)$ is the flux of α -particles with specific energy E_j , $R_\alpha(E_j)$ refers to the α -particle production rate for the decay with the energy E_j from ^{232}Th or ^{238}U decay chain. If we consider the specific activity of ^{232}Th and ^{238}U in terms of the concentration in ppm/g/y, then

$$R_\alpha(E_j) = 10^{-6} \frac{N_A}{A_a} \frac{\ln 2}{t_{1/2}} B_j, \quad (3)$$

where A_a stands for the atomic mass number of ^{232}Th or ^{238}U , B_j represents the α -particle branching ratio for a specific energy decay channel E_j , and $t_{1/2}$ is the half life of the decay.

The cross section in Eq.(2), $\int_0^{E_j} \frac{d\sigma(E_\alpha, E_n)}{dE_\alpha} dE_\alpha$, is calculated by the TALYS simulation code [32] in which the cross sections of neutron production for all possible reaction channels are calculated. The flux of α -particles is obtained by combining the production rate of α -particles with the corresponding mass stopping power in the target. The mass stopping power for specific energies is calculated by our simulation described in Ref. [35] and the ASTAR program [36]. We use the decay chains of selected isotopes in Ref. [31] for α -particle emission from ^{238}U and ^{232}Th decays. Only decays with visible energies larger than 0.1 MeV or branching ratio more than 0.5% are included.

3 Results and Discussions

The (α, n) induced neutron yield is calculated for a number of elements by using Eq.(2) and Eq.(3). The differential energy spectra of neutrons for specific target elements are listed in Tables 1 to 10 and plotted in Figures 1 to 10. Only the results for neutron energies greater than 0.1 MeV with the energy bin size of 0.1 MeV are presented. Note that the calculations with the thick target model under equilibrium conditions give the maximum contribution of the neutron yield. It's worthwhile to note that we also calculated the (α, n) neutron yield for lead. However, the result showed that there is no (α, n) neutron yield in lead due to a very high coulomb barrier which largely restricts the (α, n) reactions. The neutron yield from spontaneous ^{235}U fission is about 5% of the total neutron yields from uranium and thorium decays. Those neutrons from ^{235}U with a natural isotropic abundance of 0.72% is not included in these tables. The α -particles from samarium, a dopant of the glasses for PMTs at a level of $\sim 0.1\%$ to $\sim 1\%$ [33,34] depending on the type of glasses, have a maximum energy of 2.5 MeV. As a result, the induced neutrons are less energetic (< 5 MeV) compared to the neutrons caused by uranium and thorium decays.

We compared our results with the calculations made by Heaton *et. al.* [21], and found the total number of neutron yields in good agreement. Note that the neutron energy spectra in various elements are quite different. Neutron induced background in the region of interest for dark matter experiments is very sensitive to the neutron energy. Thus the neutron energy spectrum is very important in the Monte Carlo simulation that evaluates the neutron induced background for various dark matter experiments.

Table 1. Neutron production rate via (α, n) reaction due to natural radioactivity.

Table 2. Neutron production rate via (α, n) reaction due to natural radioactivity.

Table 3. Neutron production rate via (α, n) reaction due to natural radioactivity.

Table 4. Neutron production rate via (α, n) reaction due to natural radioactivity.

Table 5. Neutron production rate via (α, n) reaction due to natural radioactivity.

Table 6. Neutron production rate via (α, n) reaction due to natural radioactivity

Table 7. Neutron production rate via (α, n) reaction due to natural radioactivity.

Table 8. Neutron production rate via (α, n) reaction due to natural radioactivity.

Table 9. Neutron production rate via (α, n) reaction due to natural radioactivity.

Range(MeV)		$0 \sim .1$	$.1 \sim .2$	$.2 \sim .3$	$.3 \sim .4$	$.4 \sim .5$	$.5 \sim .6$	$.6 \sim .7$	$.7 \sim .8$	$.8 \sim .9$	$.9 \sim 1$	Sum	
E_n	Source	$\alpha + Si \rightarrow$ Outgoing Neutron Flux ($ppm^{-1}g^{-1}year^{-1}$)											
0	^{238}U	/	2.7e-05	5.1e-03	8.9e-03	1.4e-02	1.2e-02	1.0e-02	8.8e-03	2.8e-02	2.9e-02	1.2e-01	
	^{232}Th	/	8.6e-04	5.5e-04	1.2e-06	1.2e-06	1.2e-06	9.1e-04	9.1e-04	3.7e-04	8.2e-03	1.2e-02	
1	^{238}U	9.4e-03	2.5e-02	2.1e-02	9.4e-03	3.3e-02	2.9e-02	1.8e-03	2.4e-02	2.4e-02	1.4e-03	1.8e-01	
	^{232}Th	7.9e-03	4.8e-03	1.0e-02	5.5e-03	5.9e-03	9.7e-03	9.3e-03	1.2e-02	8.8e-03	6.6e-03	8.1e-02	
2	^{238}U	1.4e-03	2.2e-03	1.6e-03	5.5e-03	1.1e-02	1.2e-02	1.0e-02	7.1e-03	9.0e-03	3.2e-02	9.3e-02	
	^{232}Th	9.5e-03	1.6e-02	1.2e-02	2.8e-03	8.6e-03	7.4e-03	7.1e-04	4.2e-06	2.8e-05	2.2e-04	5.8e-02	
3	^{238}U	3.5e-02	2.1e-02	3.2e-02	2.6e-02	7.8e-03	3.4e-03	6.0e-03	7.8e-03	5.7e-03	2.3e-03	1.5e-01	
	^{232}Th	8.6e-04	1.9e-03	2.7e-03	3.8e-03	4.0e-03	2.4e-03	1.4e-03	1.9e-03	5.0e-03	8.1e-03	3.2e-02	
4	^{238}U	5.1e-04	5.9e-05	3.6e-06	4.1e-07	6.2e-07	8.3e-07	2.4e-06	2.5e-05	2.0e-04	9.6e-04	1.8e-03	
	^{232}Th	6.3e-03	4.4e-03	5.3e-03	4.6e-03	3.0e-03	1.8e-03	7.2e-04	1.7e-04	2.3e-05	1.7e-06	2.6e-02	
5	^{238}U	2.8e-03	5.1e-03	5.8e-03	4.2e-03	1.8e-03	5.0e-04	8.3e-05	8.2e-06	4.8e-07	1.6e-08	2.0e-02	
	^{232}Th	7.2e-08	2.8e-09	9.7e-10	7.9e-10	4.8e-09	1.0e-07	1.4e-06	1.2e-05	6.9e-05	2.4e-04	3.3e-04	
6	^{238}U	3.3e-10	3.9e-12	2.7e-14	0.0	0.0	0.0	0.0	0.0	0.0	0.0	3.4e-10	
	^{232}Th	5.6e-04	8.2e-04	7.9e-04	5.0e-04	2.0e-04	5.3e-05	8.8e-06	9.1e-07	6.0e-08	2.4e-09	2.9e-03	
> 7	^{238}U	0.0	0.0	0.0	0.0	0.0	0.0	0.0	0.0	0.0	0.0	0.0	
	^{232}Th	6.1e-11	9.5e-13	9.1e-15	0.0	0.0	0.0	0.0	0.0	0.0	0.0	6.2e-11	
Tot	^{238}U											5.5e-01	
	^{232}Th											2.1e-01	

Table 10. Neutron production rate via (α, n) reaction due to natural radioactivity.

Range(MeV)		0 ~ .1	.1 ~ .2	.2 ~ .3	.3 ~ .4	.4 ~ .5	.5 ~ .6	.6 ~ .7	.7 ~ .8	.8 ~ .9	.9 ~ 1	Sum	
E_n	Source	$\alpha + Fe \rightarrow$ Outgoing Neutron Flux ($ppm^{-1}g^{-1}year^{-1}$)											
0	^{238}U	/	7.8e-03	9.7e-03	5.4e-03	9.6e-03	9.6e-03	2.5e-04	2.6e-04	2.8e-04	3.0e-04	4.3e-02	
	^{232}Th	/	4.4e-03	5.5e-03	6.4e-03	7.3e-03	8.1e-03	9.0e-03	9.7e-03	1.5e-02	1.5e-02	8.1e-02	
1	^{238}U	3.1e-04	3.0e-04	3.0e-04	3.0e-04	3.0e-04	2.1e-02	3.1e-02	1.1e-02	1.4e-03	1.7e-03	6.7e-02	
	^{232}Th	1.0e-02	1.2e-02	1.2e-02	5.3e-03	2.7e-04	2.6e-04	2.6e-04	2.6e-04	2.5e-04	2.4e-04	4.1e-02	
2	^{238}U	2.4e-02	2.3e-02	2.4e-04	2.4e-04	2.5e-04	2.6e-04	3.3e-04	2.2e-04	4.1e-05	3.4e-05	4.9e-02	
	^{232}Th	2.2e-04	2.1e-04	2.1e-04	2.2e-04	2.1e-04	3.7e-03	7.6e-03	9.6e-03	5.8e-03	9.4e-04	2.9e-02	
3	^{238}U	3.6e-05	1.1e-04	1.7e-04	1.1e-04	8.1e-05	1.4e-04	1.8e-04	9.7e-05	1.7e-05	1.2e-06	9.4e-04	
	^{232}Th	8.8e-03	8.8e-03	9.4e-04	1.3e-04	1.3e-04	1.4e-04	1.8e-04	1.4e-04	4.1e-05	8.3e-06	1.9e-02	
4	^{238}U	1.1e-06	3.1e-06	1.5e-05	6.5e-05	1.3e-04	1.3e-04	5.5e-05	1.0e-05	7.1e-07	2.0e-08	4.1e-04	
	^{232}Th	1.3e-05	4.1e-05	7.3e-05	6.6e-05	4.5e-05	5.4e-05	7.0e-05	5.0e-05	2.0e-05	8.2e-06	4.4e-04	
5	^{238}U	2.3e-09	3.5e-09	2.4e-08	2.2e-07	1.3e-06	5.3e-06	1.4e-05	2.3e-05	2.6e-05	1.9e-05	8.9e-05	
	^{232}Th	6.0e-06	3.8e-06	5.2e-06	1.8e-05	4.0e-05	4.5e-05	2.7e-05	7.8e-06	1.1e-06	6.9e-08	1.5e-04	
6	^{238}U	9.4e-06	3.0e-06	6.1e-07	8.1e-08	6.8e-09	3.6e-10	1.2e-11	2.6e-13	3.4e-15	0.0	1.3e-05	
	^{232}Th	2.1e-09	6.1e-10	7.5e-09	6.7e-08	4.0e-07	1.6e-06	4.2e-06	7.5e-06	9.1e-06	7.6e-06	3.0e-05	
> 7	^{238}U	0.0	0.0	0.0	0.0	0.0	0.0	0.0	0.0	0.0	0.0	0.0	
	^{232}Th	4.3e-06	1.6e-06	4.2e-07	7.2e-08	8.2e-09	6.1e-10	3.0e-11	9.7e-13	2.0e-14	0.0	6.4e-06	
Tot	^{238}U											1.6e-01	
	^{232}Th											1.7e-01	

Table 11. Neutron production rate via (α, n) reaction due to natural radioactivity of samarium, specifically.

Table 12. Neutron production rate via (α, n) reaction due to natural radioactivity of samarium, specifically.

Table 13. Neutron production rate via (α, n) reaction due to natural radioactivity of samarium, specifically.

Range(MeV)	0 ~ .1	.1 ~ .2	.2 ~ .3	.3 ~ .4	.4 ~ .5	.5 ~ .6	.6 ~ .7	.7 ~ .8	.8 ~ .9	.9 ~ 1	Sum
E_n	$\alpha + B \rightarrow$ Outgoing Neutron Flux ($ppm^{-1}g^{-1}year^{-1}$)										
0	/	1.5e-10	1.9e-05	1.9e-05	1.8e-10	1.2e-09	1.0e-08	7.9e-08	5.0e-07	2.6e-06	4.1e-05
1	1.1e-05	4.1e-05	1.2e-04	2.9e-04	5.7e-04	9.4e-04	1.3e-03	1.4e-03	1.3e-03	9.8e-04	6.9e-03
2	6.1e-04	3.2e-04	1.5e-04	6.6e-05	3.7e-05	2.9e-05	2.7e-05	2.6e-05	2.4e-05	2.1e-05	1.3e-03
3	1.8e-05	1.4e-05	1.0e-05	7.3e-06	4.9e-06	3.1e-06	1.9e-06	1.1e-06	5.8e-07	3.0e-07	6.1e-05
4	1.4e-07	6.7e-08	2.9e-08	1.2e-08	4.7e-09	1.8e-09	6.2e-10	2.1e-10	6.5e-11	2.0e-11	2.6e-07
> 5	5.6e-12	1.5e-12	3.8e-13	9.2e-14	2.1e-14	4.6e-15	9.5e-16	0.0	0.0	0.0	7.6e-12
Tot											

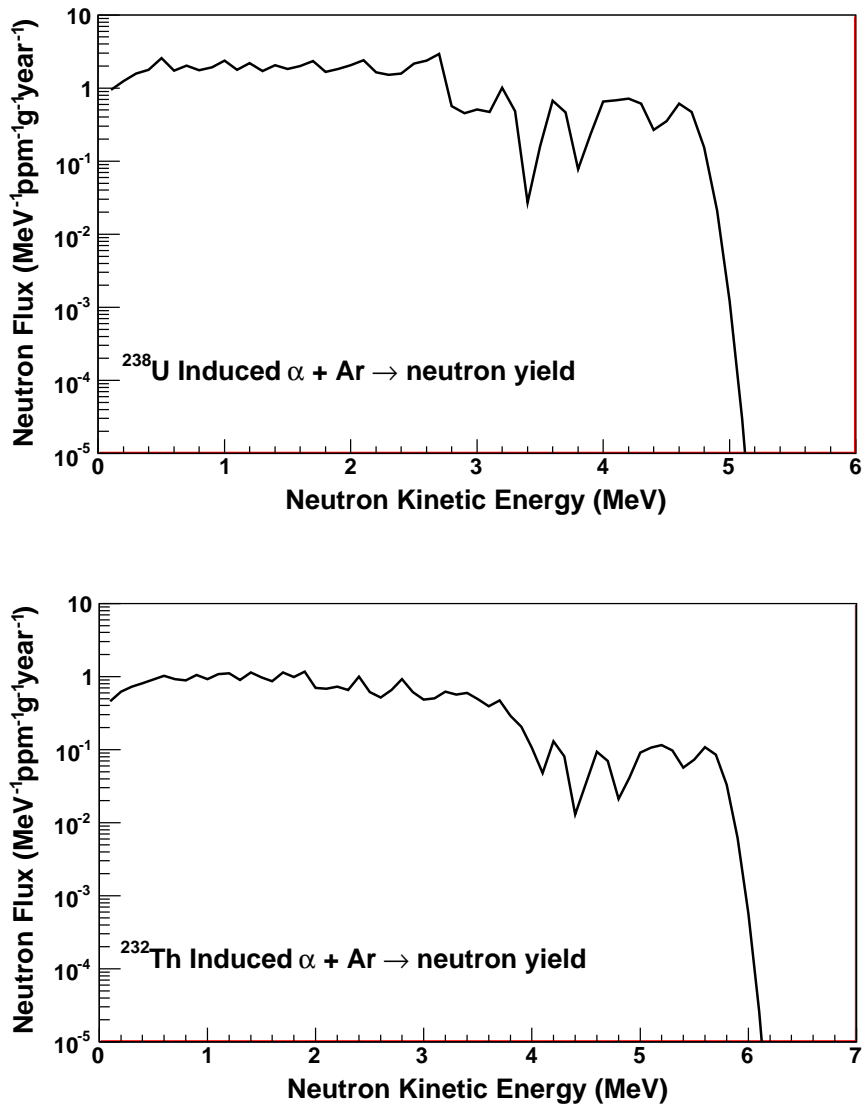


Fig. 1. The differential neutron flux induced by (α, n) reaction in a thick target of argon. The α -particles are induced by ^{238}U and ^{232}Th decays.

4 Conclusions

We have calculated the (α, n) neutron yield and energy spectrum for many elements that are used to build low background experiments. Both neutron yields and energy spectra are important to the contribution in the energy region of interest. Therefore, it is critical to have information from both in the Monte Carlo simulation to predict the possible contributions in the energy region of interest from the (α, n) neutrons. The neutron yield from many elements are compared to Heaton *et al.* [21]. Good overall agreement is obtained.

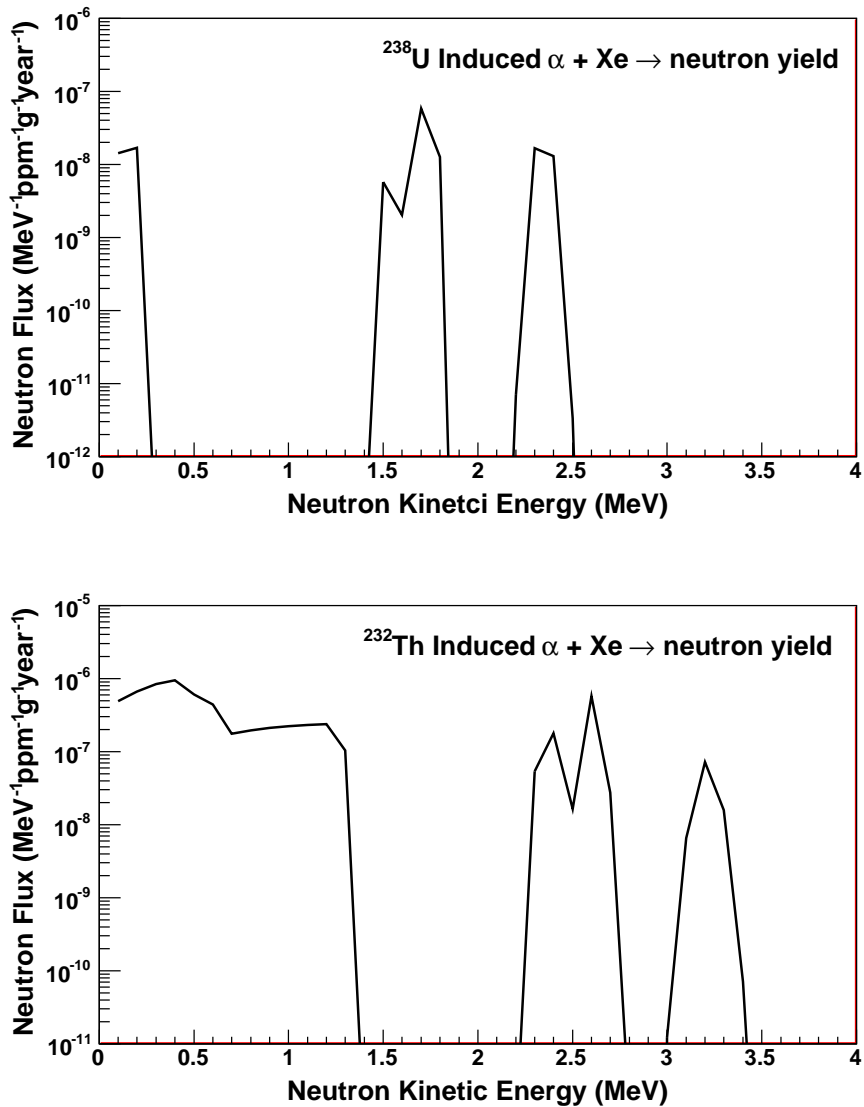


Fig. 2. The differential neutron flux induced by (α, n) reaction in a thick target of xenon. The α -particles are induced by ^{238}U and ^{232}Th decays.

5 Acknowledgment

The authors wish to thank Yongchen Sun and Christina Keller at The University of South Dakota for the invaluable support that made this work successful. This work was supported in part by the NSF grant 0758120, the Office of Research at The University of South Dakota, and by Laboratory Directed Research and Development at Los Alamos National Laboratory.

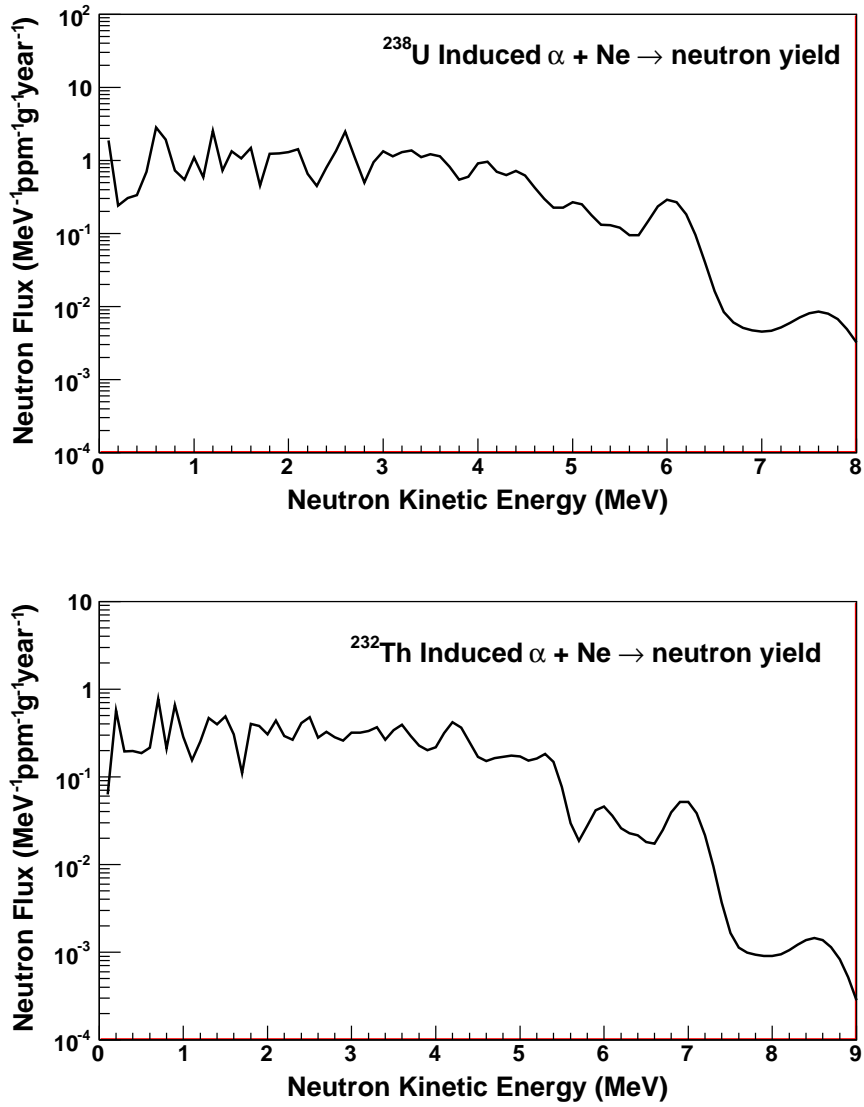


Fig. 3. The differential neutron flux induced by (α, n) reaction in a thick target of neon. The α -particles are induced by ^{238}U and ^{232}Th decays.

References

- [1] D. N. Spergel *et al.*, *Astrophys. J. Suppl. Ser.* **148**, 175 (2003).
- [2] W. Freeman and M. Turner, *Rev. Mod. Phys.* **75**, 1433 (2003).
- [3] M. W. Goodman and E. Witten, *Phys. Rev. D* **31**, 3059 (1985).
- [4] G. Jungman, M. Kamionkowski, and K. Griest, *Phys. Rep.* **267**, 195 (1996).
- [5] D. S. Akerib *et al.* (CDMS Collaboration), *Phys. Rev. Lett.* **93**, 211301 (2004).
- [6] A. Benoit *et al.* (EDELWEISS Collaboration), *Phys. Lett. B* **545**, 43 (2002).

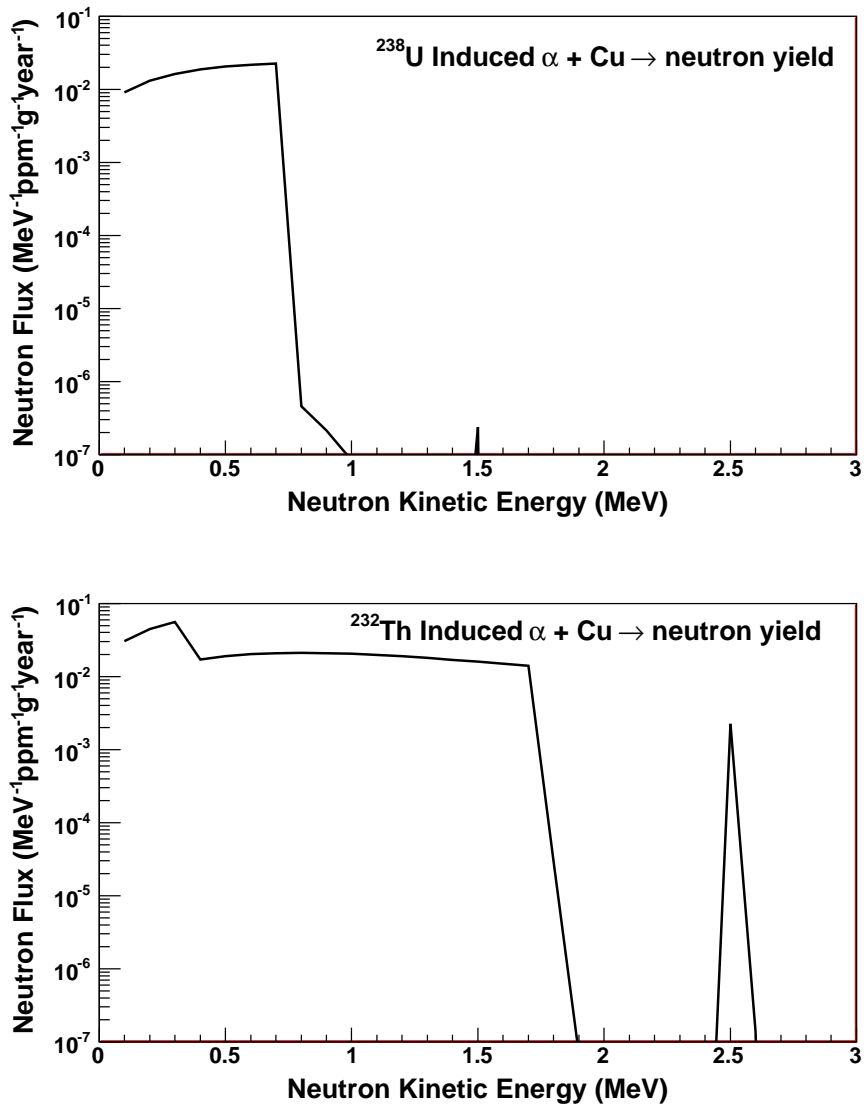


Fig. 4. The differential neutron flux induced by (α, n) reaction in a thick target of copper. The α -particles are induced by ^{238}U and ^{232}Th decays.

- [7] J. Angle *et al.* (XENON10 Collaboration), Phys. Rev. Lett. **100**, 021303 (2008).
- [8] P. Benetti *et al.*, Astroparticle Physics, V **28**, 495 (2008).
- [9] R. Bernabei *et al.* (DAMA Collaboration), Phys. Lett. **B 480**, 23 (2000).
- [10] G. Angloher *et al.*, Astropart. Phys. **18**, 43 (2002).
- [11] M. Barnabe-Heider *et al.* (PICASSO), Phys. Lett. **B 624**, 186 (2005).
- [12] G. J. Alner *et al.* (UKDMC), Phys. Lett. **B 616**, 17 (2005).
- [13] V. A. Kudryavtsev (UKDMC), in the Fifth International Workshop on the Identification of Dark Matter, Edinburgh, Scotland, 2004.

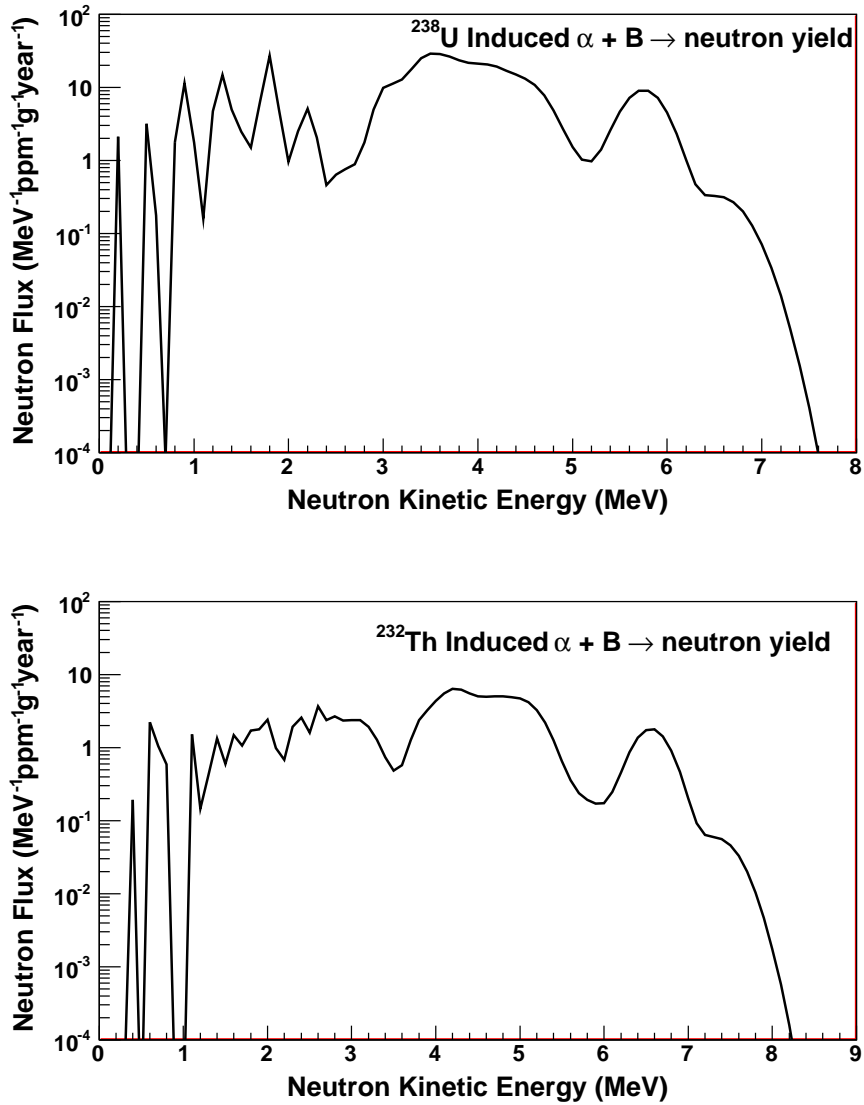


Fig. 5. The differential neutron flux induced by (α, n) reaction in a thick target of boron. The α -particles are induced by ^{238}U and ^{232}Th decays.

- [14] R. Bernabei *et al.* (DAMA Collaboration), Riv. N. Cim. **26** (2003) 1-73.
- [15] R. Bernabei *et al.* (DAMA Collaboration), arXiv:0804.2741v1.
- [16] Z. Ahmed et al., (CDMS Collaboration), pre-print, astro-ph/0802.3530
- [17] D. West and A. C. Sherwood, Ann. Nucl. Eng. **9**, 551 (1982).
- [18] J. K. Bai and J. Gomez del Campo, Nucl. Sci. Eng. **71**, 18 (1978).
- [19] H. Lisien and A. Paulsen, Atomkernenergie **30**, 1 (1970).
- [20] Y. Feige, B. G. Oltman, and J. Kastner, J. Geophys. Res. **73**, 3135 (1968).
- [21] R. Heaton *et al.*, Nucl. Geophys. V **4**, 499 (1990).

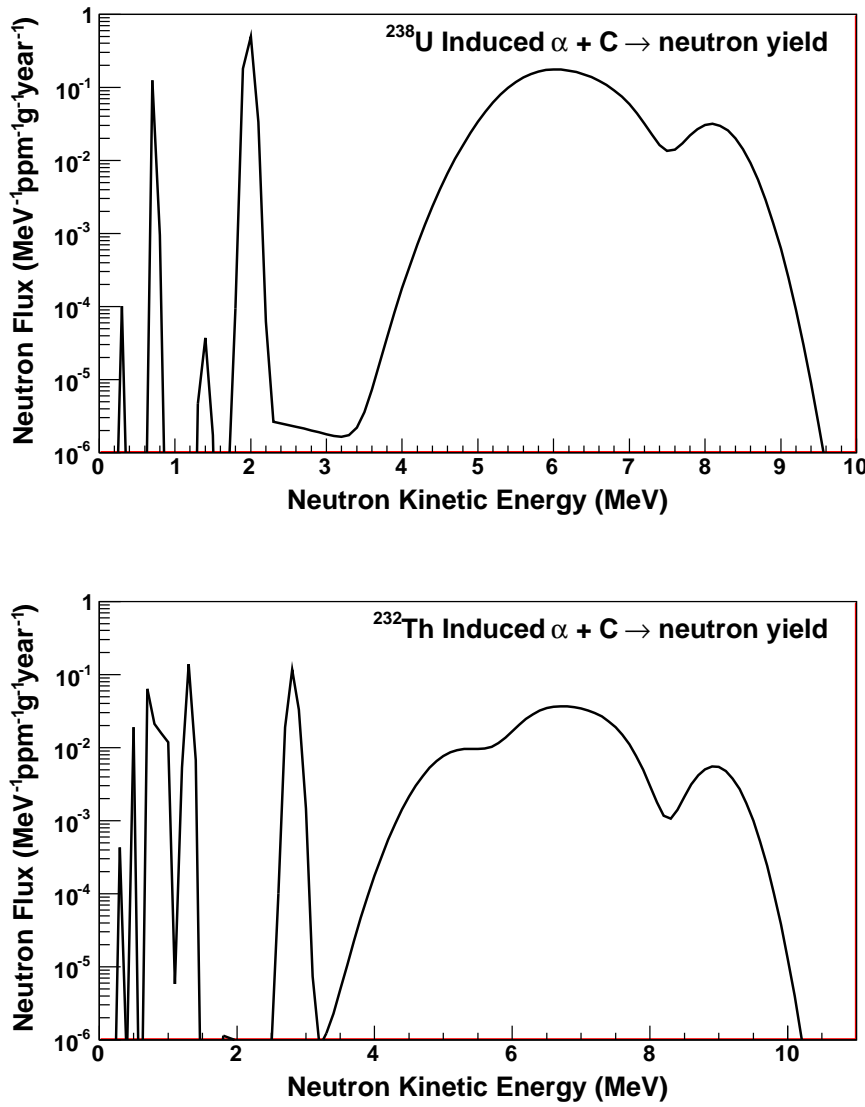


Fig. 6. The differential neutron flux induced by (α, n) reaction in a thick target of carbon. The α -particles are induced by ^{238}U and ^{232}Th decays.

- [22] R. Heaton *et al.*, Nucl. Instrum. Methods Phys. Res. A **276**, 529 (1989).
- [23] S. Harissopoulos *et al.*, Phys. Rev. C **72**, 062801 (2005).
- [24] G. J. H. Jacobs and H. Liskien, Ann. nucl. Energy, **10**, 541 (1983).
- [25] J. H. Gibbons and R. L. Macklin, Phys. Rev. **114**, 571 (1959).
- [26] W. Fitz, F. Kienle, R. Maschuw, and B. Zeitnitz, Phys. Rev. C **14**, 755 (1976).
- [27] L. Van Der Zwan and K. W. Geiger, Nucl. Phys. A **246**, 93 (1975).
- [28] Eric B. Norman, Timothy E. Chupp, Kevin T. Lesko, Peter Schwalbach, and Patrick J. Grant, Nucl. Phys. A **390**, 561 (1982).

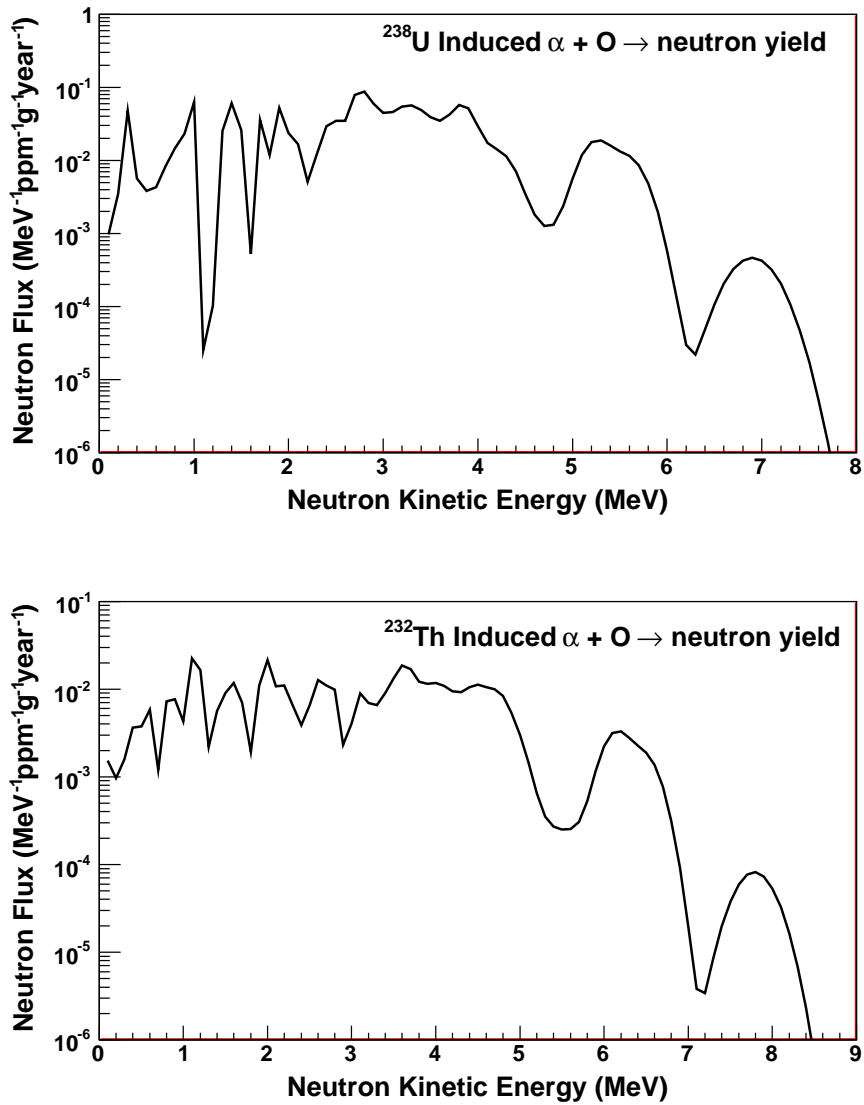


Fig. 7. The differential neutron flux induced by (α, n) reaction in a thick target of oxygen. The α -particles are induced by ^{238}U and ^{232}Th decays.

- [29] Eric B. Norman, Timothy E. Chupp, Kevin T. Lesko, Patrick J. Grant, and Gene L. Woodruff, Phys. Rev. C **30**, 1339 (1984).
- [30] R. K. Heaton, H. W. Lee, B. C. Robertson, E. B. Norman, K. T. Lesko, and B. Sur, NIM A **364** (1995), 317.
- [31] D. S. Delion, A. Insolia, and R. J. Liotta, Nucl. Phys. (Supplement) A **654**, 673c (1999). A. M. Sanchez and P. R. Montero, Nucl. Instrum. Methods Phys. Res. A **420**, 481 (1999).
- [32] A. J. Koning, S. Hilaire and M. C. Duijvestijn, “TALYS: Comprehensive nuclear reaction modeling,” Proceedings of the International Conference on Nuclear Data for Science and Technology - ND2004, AIP vol. 769, eds. R. C. Haight, M.

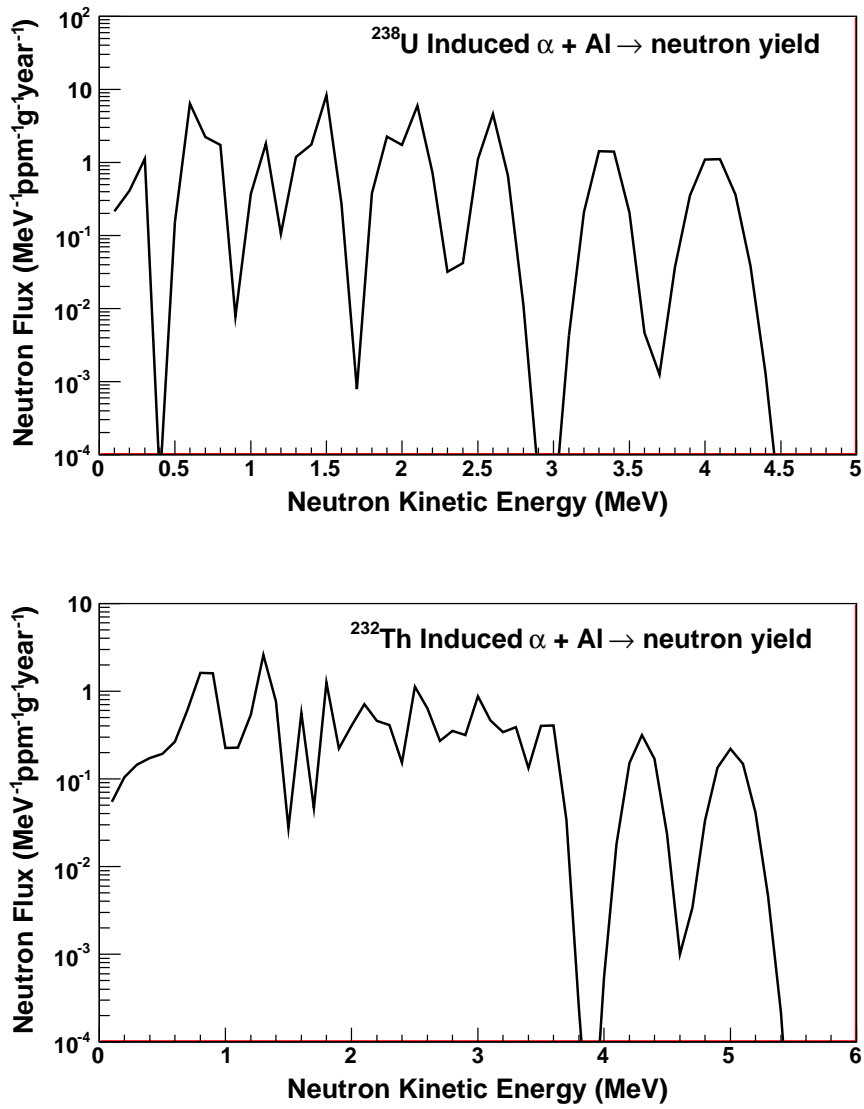


Fig. 8. The differential neutron flux induced by (α, n) reaction in a thick target of aluminum. The α -particles are induced by ²³⁸U and ²³²Th decays.

B. Chadwick, T. Kawano, and P. Talou, Sep. 26-Oct. 1, 2004, Sante Fe, USA, 2005, pp. 1154.

- [33] Andreas Hermann and Doris Ehrt, Journal of Non-Crystalline Solids, V 354, 916 (2008).
- [34] M. S. Iovu *et al.*, Journal of Optoelectronics and Advanced Materials V 8, 1341 (2006).
- [35] D.-M. Mei *et al.*, Astroparticle Physics 30, (2008) 12-17.
- [36] <http://physics.nist.gov/PhysRefData/Star/Text/ASTAR.html>.

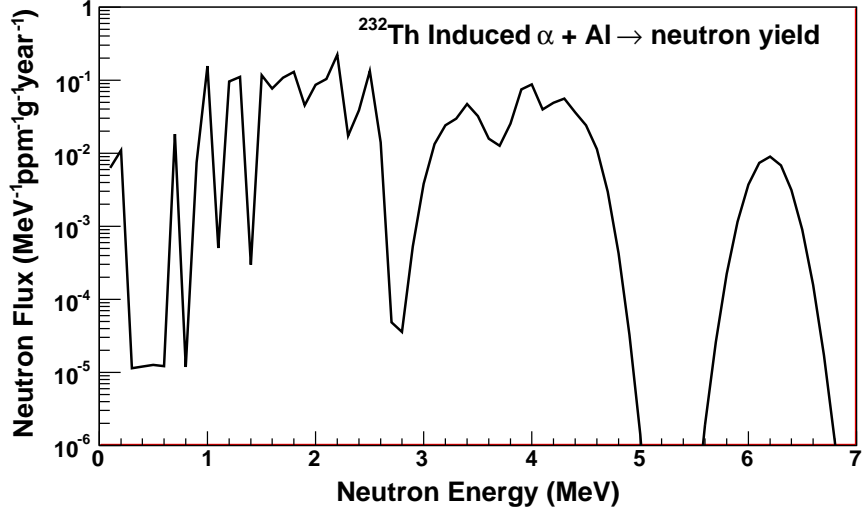
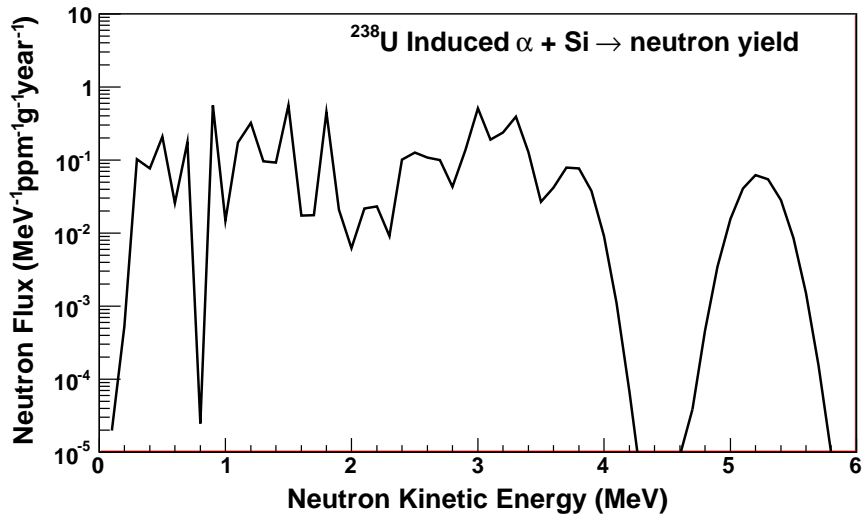


Fig. 9. The differential neutron flux induced by (α, n) reaction in a thick target of silicon. The α -particles are induced by ^{238}U and ^{232}Th decays.

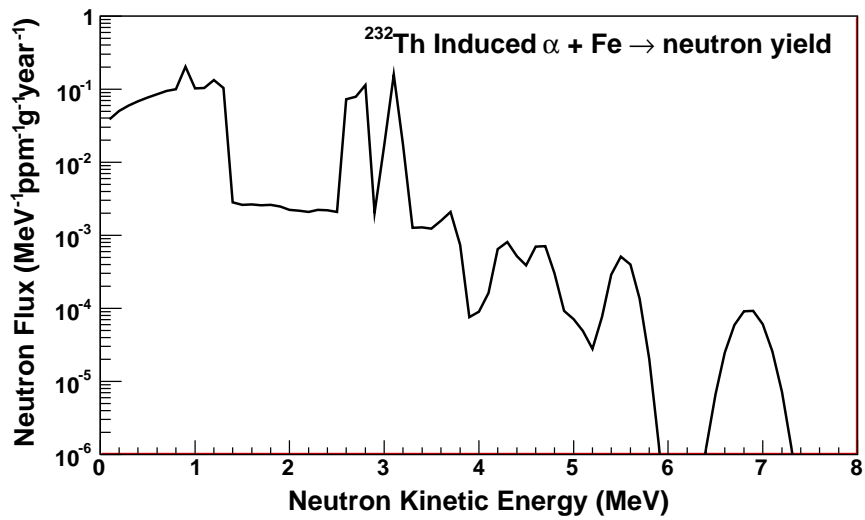
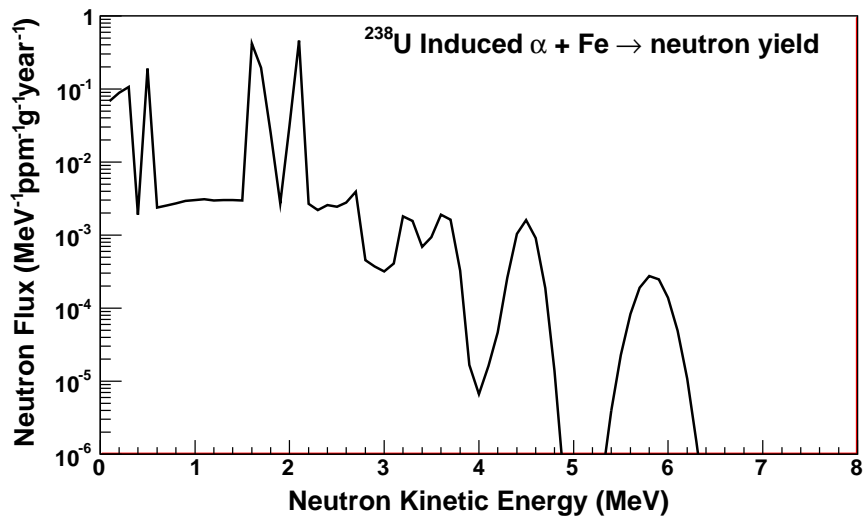


Fig. 10. The differential neutron flux induced by (α, n) reaction in a thick target of iron. The α -particles are induced by ^{238}U and ^{232}Th decays.

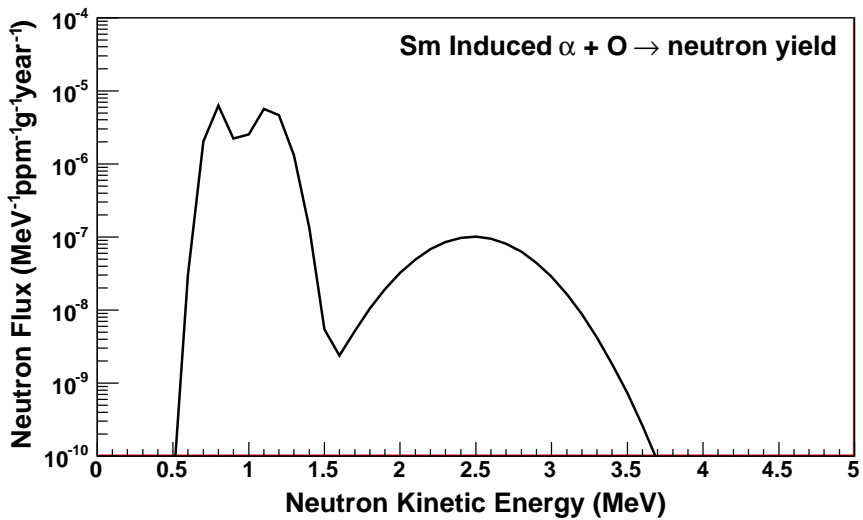


Fig. 11. The differential neutron flux induced by (α, n) reaction in a thick target of oxygen. The α -particles are induced by samarium decays.

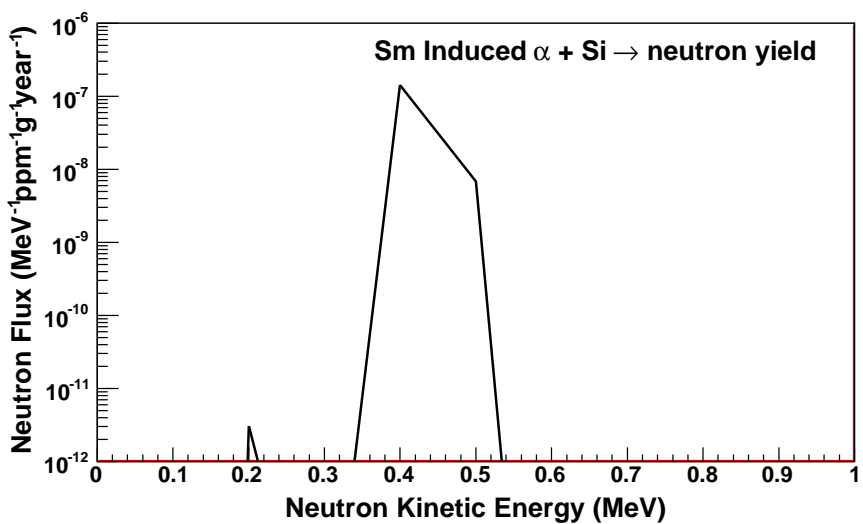


Fig. 12. The differential neutron flux induced by (α, n) reaction in a thick target of silicon. The α -particles are induced by samarium decays.

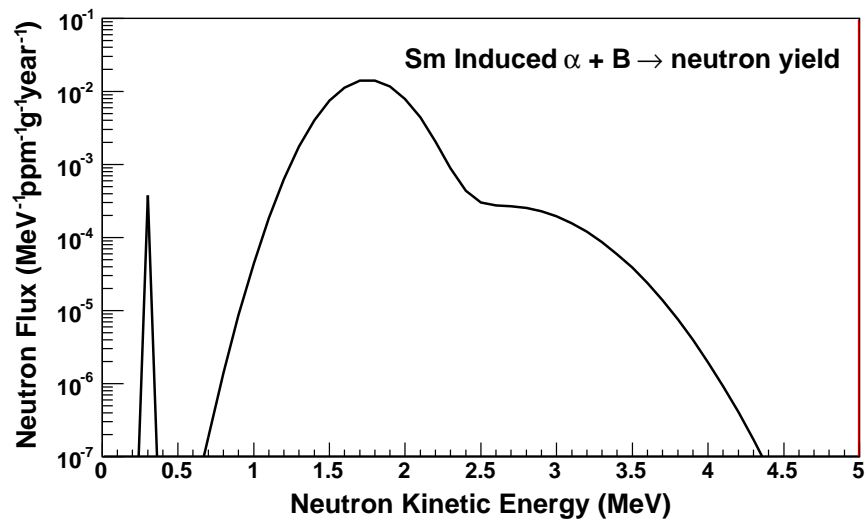


Fig. 13. The differential neutron flux induced by (α, n) reaction in a thick target of boron. The α -particles are induced by samarium decays.